Spatially Resolved STIS Spectra of Betelgeuse's Outer Atmosphere

A. Lobel, J. Aufdenberg, A. K. Dupree, R. L. Kurucz, R. P. Stefanik, & G. Torres

Harvard-Smithsonian Center for Astrophysics, Cambridge, MA, USA

Summary

We present spatially resolved spectra observed with the Space Telescope Imaging Spectrograph on the Hubble Space Telescope of the upper chromosphere and dust envelope of α Orionis (M2 Iab). In the fall of 2002 a set of five high-resolution near-UV spectra was obtained by scanning at intensity peak-up position and four off-limb target positions up to one arcsecond, using a small aperture (200 by 63 mas) to investigate the thermal conditions and flow dynamics in the outer atmosphere of this important nearby cool supergiant star.

Based on Mg II h & k, Fe II, C II, and Al II emission lines we provide the first evidence for the presence of warm chromospheric plasma at least 1 arcsec away from the star at $\sim$40 R_* (1 $R_*\simeq$700 $R_\odot$). The STIS spectra reveal that Betelgeuse's upper chromosphere extends far beyond the circumstellar Hα envelope of $\sim$5 R_*, determined from previous ground-based imaging.

The flux in the broad and self-absorbed resonance lines of Mg II decreases by a factor of $\sim$700 compared to the flux at chromospheric disk center. We observe strong asymmetry changes in the Mg II h and Si I line profiles when scanning off-limb, signaling outward acceleration of gas outflow in the upper chromosphere.

From the radial intensity distributions of Fe I and Fe II emission lines we determine the radial non-LTE iron ionization balance. We compute that the local kinetic gas temperatures of the warm chromospheric gas component in the outer atmosphere exceed 2600 K when assuming local gas densities of the cool gas component, determined from our radiative transfer models that fit the 9.7 μm silicate dust emission feature. The spatially resolved STIS spectra directly demonstrate that warm chromospheric plasma co-exisists with cool gas in Betelgeuse's circumstellar dust envelope.

This reseach is based on data obtained with the NASA/ESA Hubble Space Telescope, collected at the STScI, operated by AURA Inc., under contract NAS5-26555. Financial support is provided by STScI grant HST-GO-09369.01 to the Smithsonian Astrophysical Observatory.

1. STIS Observations

STIS spectra of the red supergiant α Ori have been observed for GO 9369 in HST Cycle 11; *A direct Test for Dust-driven Wind Physics*. This program investigates the detailed acceleration mechanisms of wind outflow in the outer atmospheres (chromosphere and dust envelope) of cool stars. Using the exceptional capabilities of HST-STIS we observe the UV spectrum with $\lambda/\Delta\lambda\simeq$33,000 between 2275 Å and 3180 Å with spatially resolved scans across the chromospheric disk at 0, 200, 400, 600, & 1000 mas (Visit 1), at 0 & 2000 mas (Visit 2), and at 0 & 3000 mas (Visit 3). We presently discuss the spectra observed in fall 2002 of Visit 1. The spectra of Visits 2 & 3 of spring 2003 will be presented later. Exposure times range from 500 s at 200 mas to 7200 s at 1", yielding good S/N$\geq$20. The spectra are calibrated with CALSTIS v2.12 using the most recently updated calibration reference files. Wavelength calibration accuracies are better than $\sim$1 detector pixel or 1.3 km s^{-1}.

2. Si I λ2516 line profile changes

In previous work we modeled the detailed shape of the Si I λ2516 resonance emission line (Lobel & Dupree 2001, ApJ 558, 815). The line has previously been observed by scanning over the inner chromosphere at 0, 25, 50, and 75 mas, using a slit size of 100 $\times$ 30 mas. The right-hand figure shows the Si I line profiles and the respective slit positions compared to the near-UV continuum (in false colors) observed with HST-FOC. The double-peaked line profiles across the inner chromosphere were observed in March 1999. The central (self-) absorption core results from scattering opacity in the chromosphere. The asymmetry of the emission component intensities probes the chromospheric flow dynamics in our line of sight. The spectra of GO 9369 are observed across the outer chromosphere using a slitsize of 200 $\times$ 63 mas. These profiles *appear* red-shifted with a rather weak short-wavelength emission component. It signals substantial wind outflow opacity in the upper chromoshere, which fastly accelerates beyond 200 mas ($\simeq$8.1 R_*).

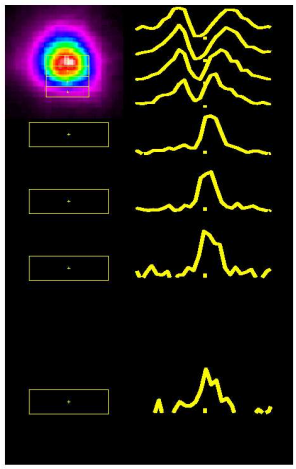

3. Mg II k & h line profile changes

The right-hand figure shows the detailed profiles of the Mg II h & k lines observed up to 1000 mas. The emission line intensities decrease by a factor of $\sim$700 from chromospheric disk center (TP 0) to 1". These optically thick chromospheric lines show remarkable changes of their detailed shapes when scanning off-limb. The full width across both emission components at half intensity maximum decreases by $\sim$20%, while the broad and saturated central absorption core narrows by more than 50%. Beyond 600 mas the central core assumes a constant width which results from absorption contributions by the local interstellar medium ($d_*\simeq$132 pc). We observe a strong increase of the (relative) intensity of the long-wavelength emission component in both lines beyond 200 mas. It signals fast wind acceleration beyond this radius. Note that the short-wavelength emission components of the k and h lines are blended with chromospheric Mn I lines (decreasing the k- and increasing the h-component), but that become much weaker in the outer chromosphere.

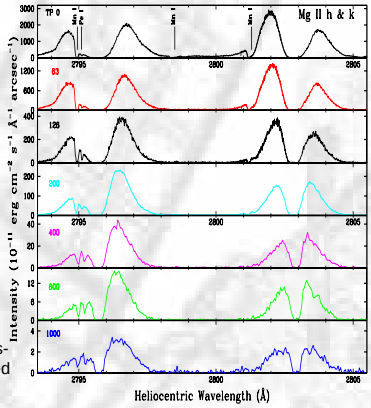

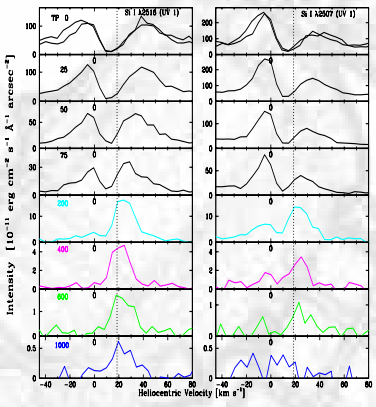

4. Wind Acceleration in the Upper Chromosphere

The left-hand figure compares the profiles of the Si I λ2516 and λ2507 resonance lines (vertical dotted lines are drawn at stellar rest velocity). Both lines share a common upper energy level and their intensities are influenced by pumping through a fluoresced Fe II line. The self-absorption cores of the Si I lines are therefore observed far out, into the upper chromosphere. The shape of these unsaturated emission lines is strongly opacity sensitive to the local chromospheric velocity field. As for the Mg II lines, the outward decreasing intensity of the short-wavelength emission component signals fast acceleration of chromospheric outflow in the upper chromosphere. We also observe this decrease for the resonance line of Mg I λ2852 (not shown). Our previous radiative transfer modeling work based on Si I revealed that α Ori's inner chromosphere oscillates non-radially, with simultaneous up- and downflows in Sept 1998. Radiative transfer modeling to determine the detailed wind structure in the outer chromosphere is underway.

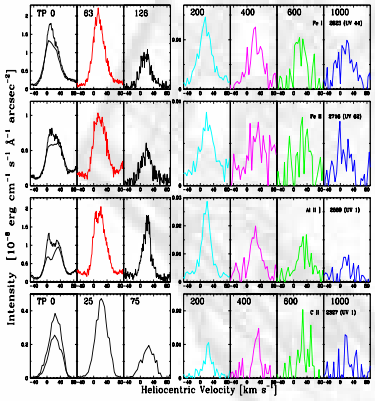

5. Ion lines in the Upper Chromosphere

We also observe ion lines of Fe II, Al II, and C II out to 1" in the upper chromosphere. The left-hand figure shows (scaled) emission lines of Fe II λ2716 (UV 62), Al II] λ2669 (UV 1), and C II λ2327 (UV 1). The Fe I λ2823 (UV 44) line is also shown for comparison (top panels). The lines at the inner chromosphere are observed in April 1998 (thin drawn lines) with R$\sim$114,000 at TPs 0, 63, and 126 mas, while the lines of the outer chromosphere are observed with medium resolution in fall 2002 (boldly drawn lines). Both raster scans are however observed with the same slitsize of 200 $\times$ 63 mas so that the line intensity changes can be compared. For this purpose we select unblended lines without central self-absorption cores that become sufficiently optically thin in the outer chromosphere, and that are significantly observed against the local background noise level.

6. Radial Intensity Distribution of Ion Lines

We wavelength integrate the selected chromospheric emission lines and the Mg II lines beyond the line wings. Their radial intensity distributions I(r) are compared in the right-hand figure. The intensity errorbars are derived from the STIS pipeline flux calibration errors, while the radius errorbars are derived from the projected slitwidth. We observe that the I(r) of optically thin emission from neutral and ion lines are very similar across the chromosphere. Neutral emission lines are generally observed farther out with larger S/N compared to the ion lines, but their I(r) do not differ significantly within the errors. We find a best fit for I(r)$\simeq$const $\times$ r^{-2}. The I(r) of the optically thick and self-absorbed Mg II lines differs significantly with I(r)$\simeq$const $\times$ r$^{-2.7}$. The steeper intensity distribution signals important radiative transfer effects for the shapes of the stronger Mg II lines (see 3).

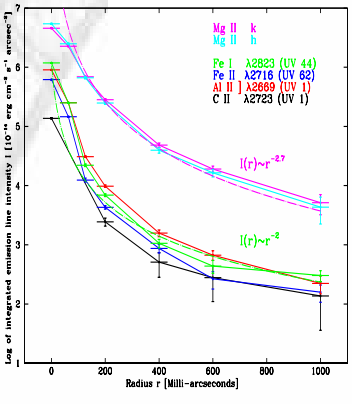

7. Radial Non-LTE Iron Ionization Balance

In the upper panel of the right-hand figure we compute the iron ionization fraction from the I(r) of the Fe I and Fe II lines. The intersection of the curves (at dots) provides the excitation temperature corresponding to the observed line intensity ratios for spontaneous emission. We compute iron ionization fractions between 99.3% and 99.7% for kinetic gas temperatures between 2600 K and 5800 K, using local gas densities $10^{-17}\leq\rho\leq10^{-15}$ gr cm^{-3} (lower panel). This temperature range corresponds to a diluted radiation field with $T_{\rm rad}\simeq$3000 K (full drawn lines), typical for the outer chromosphere. The graphs are computed with volume filling factors ϕ for warm plasma of 5% (dots) and 30% (triangles). Hydrogen is almost neutral for these conditions in the upper chromosphere. We model the circumstellar dust envelope (CDE) with radiative transfer in spherical geometry using DUSTY. A best fit to the IRAS silicate dust emission feature at 9.7 μm yields a dust condensation radius of $R_c\simeq$573 mas, where $\rho_{\rm gas}\sim5\ 10^{-16}$ gr cm^{-3} for the cool ambient gas, with temperatures below $T_{\rm dust}\leq$600 K (lower panels). The upper panel shows the temperature structure for warm chromospheric plasma computed at this $\rho_{\rm gas}$ with ϕ= 1% and 100% (solid red lines). The inner chromosphere is computed with radiative transfer fits to Hα (Lobel & Dupree 2000, ApJ 545, 454). We find that temperatures of the warm chromospheric plasma cannot decrease to below 2600 K in the CDE. Hence warm chromospheric plasma must co-exisit with cool gas of $T\leq$600 K beyond 600 mas.

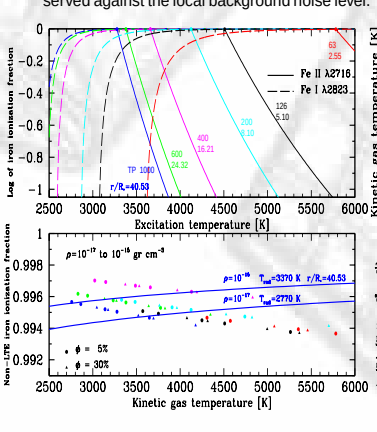

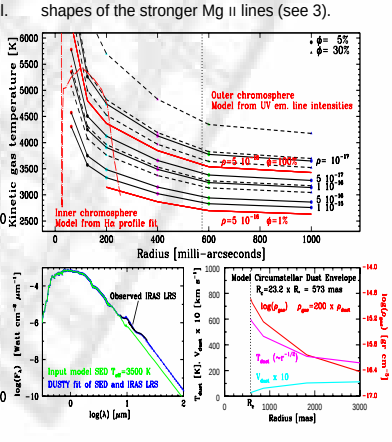

Conclusions

Warm chromospheric plasma seen at 40 R_*.
It must co-exist with cool gas of dust envelope.
Outer chromosphere shows wind acceleration.